Efficient encapsulation of antisense oligonucleotides in lipid vesicles using ionizable aminolipids: formation of novel small multilamellar vesicle structures

Sean C. Semple [a],*, Sandra K. Klimuk [b], Troy O. Harasym [a], Nancy Dos Santos [a], Steven M. Ansell [a], Kim F. Wong [b], Norbert Maurer [b], Holger Stark [c], Pieter R. Cullis [a,b], Michael J. Hope [a], Peter Scherrer [a]

[a] *Inex Pharmaceuticals Corp., 100-8900 Glenlyon Parkway, Glenlyon Business Park, Burnaby, B.C., Canada V5J 5J8*
[b] *University of British Columbia, Department of Biochemistry and Molecular Biology, 2146 Health Sciences Mall, Vancouver, B.C., Canada V6T 1Z3*
[c] *Institute for Molekularbiologie und Tumorforschung, Emil-Mannkopff-Strasse 2, 35037 Marburg, Germany*

Abstract

Typical methods used for encapsulating antisense oligodeoxynucleotides (ODN) and plasmid DNA in lipid vesicles result in very low encapsulation efficiencies or employ cationic lipids that exhibit unfavorable pharmacokinetic and toxicity characteristics when administered intravenously. In this study, we describe and characterize a novel formulation process that utilizes an ionizable aminolipid (1,2-dioleoyl-3-dimethylammonium propane, DODAP) and an ethanol-containing buffer system for encapsulating large quantities (0.15–0.25 g ODN/g lipid) of polyanionic ODN in lipid vesicles. This process requires the presence of up to 40% ethanol (v/v) and initial formulation at acidic pH values where the DODAP is positively charged. In addition, the presence of a poly(ethylene glycol)-lipid was required during the formulation process to prevent aggregation. The 'stabilized antisense-lipid particles' (SALP) formed are stable on adjustment of the external pH to neutral pH values and the formulation process allows encapsulation efficiencies of up to 70%. ODN encapsulation was confirmed by nuclease protection assays and ^{31}P NMR measurements. Cryo-electron microscopy indicated that the final particles consisted of a mixed population of unilamellar and small multilamellar vesicles (80–140 nm diameter), the relative proportion of which was dependent on the initial ODN to lipid ratio. Finally, SALP exhibited significantly enhanced circulation lifetimes in mice relative to free antisense ODN, cationic lipid/ODN complexes and SALP prepared with quaternary aminolipids. Given the small particle sizes and improved encapsulation efficiency, ODN to lipid ratios, and circulation times of this formulation compared to others, we believe SALP represent a viable candidate for systemic applications involving nucleic acid therapeutics. © 2001 Elsevier Science B.V. All rights reserved.

Keywords: Antisense oligonucleotide; Phosphorothioate; Liposome; Cationic lipid; Drug delivery; Formulation

1. Introduction

Nucleic acid-based therapeutics, such as antisense oligodeoxynucleotides (ODN), ribozymes, and plasmid DNA, offer the potential to specifically target

---

* Corresponding author. Tel.: +1-604-419-3200;
Fax: +1-604-419-3203; E-mail: ssemple@inexpharm.com

diseased cells at the molecular level. However, these large polyanionic macromolecules possess several inherent characteristics that restrict their pre-clinical and clinical utility for the therapy of chronic diseases, including cost and production of clinical grade material [1], degradation and inactivation by nucleases in plasma and cells [2], poor intracellular delivery [3,4], rapid plasma elimination [5,6], as well as renal and dose-limiting hemodynamic toxicities [7–9]. For antisense ODN, which are furthest along in clinical development, nuclease sensitivity has been minimized through chemical modifications to the nucleic acid backbones and/or sugars [10], while hemodynamic toxicities have been reduced through the use of repeated, slow infusions (2 h) or continual infusion protocols of up to 21 days [11]. However, it would be expected that encapsulation of antisense ODN and other DNA- and RNA-based therapeutics in lipid vesicles would greatly reduce these concerns and improve the utility of these molecules without the need for chemical modification. This will be particularly critical for larger DNA and RNA agents such as ribozymes and plasmids on which modifications would be increasingly more complicated and costly.

Conventional and sterically stabilized liposomes have been used extensively to increase the therapeutic index of a variety of drugs by changing their pharmacokinetic and pharmacodynamic characteristics [12–14]. Lipid-based formulations of vincristine, doxorubicin, daunorubicin and amphotericin B have all demonstrated significant clinical improvement over the free compounds [12,13,15,16]. Recently, considerable effort has been applied to formulating DNA- and RNA-based therapeutics in lipid delivery systems in an attempt to realize similar benefits [3,17,18]. The development of liposome and lipid delivery systems for nucleic acid-based therapeutics for systemic therapy, however, has been limited by two principal factors – low encapsulation efficiency (< 10%) and drug to lipid ratios (0.001–0.1, w/w) in neutral lipid formulations, and pharmacokinetic and toxicity issues associated with the use of cationic lipid.

In an effort to improve encapsulation efficiencies, several approaches have been employed to entrap antisense ODN in lipid vesicles. These include direct rehydration of lipid films in the presence of nucleic acid, a minimal volume entrapment (MVE) technique, detergent dialysis, reverse-phase encapsulation, chemical modification to increase the lipophilicity of ODN, and the use of cationic lipids (reviewed in [19–21]). The inclusion of cationic lipids in lipid formulations improves the association with polyanionic nucleic acids. Moreover, the presence of a net positive surface charge on nucleic acid/lipid particles facilitates binding and uptake by cells in vitro [3]. However, in using cationic lipids it is often not clear whether all of the nucleic acid is encapsulated inside a bilayer envelope or whether small complexes of cationic liposome/nucleic acid are formed. Furthermore, when delivery systems bearing a net cationic charge are administered intravenously (i.v.), they exhibit rapid plasma clearance, distribute into lung, liver and spleen [22–24], and often exhibit liver and hemodynamic toxicities, such as activation of complement and prolongation of clotting times [25–27]. Therefore, there is a growing need to mask or reduce the cationic lipid content in delivery systems. In this study, we describe a novel process that utilizes an ionizable aminolipid to facilitate efficient encapsulation of antisense ODN in lipid vesicles that can subsequently be rendered neutral at physiological pH. Using this approach, we address the issues of improving encapsulation efficiencies and drug to lipid ratios, as well as reducing the net cationic lipid content of the vesicles, resulting in improved pharmacokinetics of the formulation relative to delivery systems containing quaternary aminolipids or cationic liposome/ODN complexes.

2. Materials and methods

2.1. Lipids and chemicals

Distearoylphosphatidylcholine (DSPC), egg phosphatidylcholine (EPC), and dioleoyldimethylammonium chloride (DODAC) were purchased from Northern Lipids, Inc. (Vancouver, B.C., Canada). 1,2-Dioleoyl-3-dimethylammonium propane (DODAP) was obtained from Avanti Polar Lipids, Inc. (Alabaster, AL, USA). Cholesterol (CH) was purchased from Sigma-Aldrich (Oakville, Ont., Canada). Radiolabeled cholesterylhexadecylether (CHE) was purchased from Mandel Scientific (Guelph, Ont.,

Canada). 1-*O*-(2′-(w-methoxypolyethyleneglycol)suc-cinoyl)-2-*N*-myristoylsphingosine (PEG-CerC$_{14}$) and 1-*O*-(2′-(w-methoxypolyethyleneglycol)succinoyl)-2-*N*-arachidoylsphingosine (PEG-CerC$_{20}$) were synthe-sized as described elsewhere [28]. All lipids were >99% pure.

2.2. Antisense ODN

All ODN were synthesized with phosphorothioate (PS) backbone chemistry. The 5′–3′ sequences and mRNA targets of these ODN are as follows: EGFR (human epidermal growth factor receptor), CCGTGGTCATGCTCC [29]; c-myc (human/mur-ine c-myc proto-oncogene), TAACGTTGAGGGG-CAT [30]; hICAM (human intercellular adhesion molecule-1), GCCCAAGCTGGCATCCGTCA [31]; mICAM (murine intercellular adhesion molecule-1), TGCATCCCCCAGGCCACCAT [32]; and sICAM (scrambled control for mICAM), TCGCATC-GACCCGCCCACTA [32]. Radiolabeled ([^{3}H] and [^{35}S]) ODN were purchased from TriLink BioTech-nologies, Inc. (San Diego, CA, USA). Early experi-ments were conducted using ICAM-1 sequences pro-vided by Dr. Frank Bennett of ISIS Pharmaceuticals (Carlsbad, CA, USA). Later work employed ODN purchased from Hybridon Specialty Products (Wor-cester, MA, USA). Extinction coefficients were calcu-lated from the pairwise extinction values for individ-ual nucleotides, taking into account nearest neighbor interactions. The purity of all ODN was determined by the individual suppliers using high performance liquid chromatography (HPLC) and/or capillary gel electrophoresis.

2.3. Preparation of stabilized antisense-lipid particles (SALP)

To determine the influence of ethanol on encapsu-lation of ODN, lipid films were hydrated with solu-tions of ODN containing varying amounts of ethanol in citrate buffer, pH 4.0. The resulting solution was then extruded through three stacked 100 nm polycar-bonate filters (Osmonics, Livermore, CA, USA) us-ing a thermobarrel extruder (Lipex Biomembranes, Vancouver, B.C., Canada) maintained at approxi-mately 65°C [33]. In the presence of ethanol, extru-sion was rapid and required low nitrogen pressures;

therefore, three filters were used to ensure a homo-geneous particle size distribution of the final vesicles. For all subsequent studies, lipid stock solutions were prepared in 100% ethanol. Typically, 13 μmol (∼10 mg) of total lipid (0.4 ml total volume) was added to a glass tube containing trace amounts of [^{14}C]CHE. ODN (2 mg by A_{260}) and trace amounts of [^{3}H]ODN were dissolved in 0.6 ml of 300 mM citric acid, pH 4.0 in a separate tube. The ODN and lipid solutions were warmed for 2–3 min to 65°C and the lipids were slowly added to the ODN, while mixing constantly. The mixture was passed 10 times through three stacked 100 nm polycarbonate filters as described above. The preparation was dialyzed (12–14 kDa cutoff) against 300 mM citrate buffer, pH 4.0 for approximately 1 h to remove excess ethanol; then further dialyzed against HBS (20 mM HEPES, 145 mM NaCl, pH 7.6) for 12–18 h to remove the citrate buffer, neutralize the DODAP and release any ODN that was associated with the surface of the vesicles. Non-encapsulated ODN was removed by DEAE-Sepharose CL-6B column chromatography. The mean diameter and size distribution of SALP was determined using a NICOMP Model 370 Sub-micron particle sizer, and was typically 110 ± 30 nm. A typical 1.0 ml formulation consisted of 13 μmol (∼10 mg) total of DSPC/CH/DODAP/PEG-CerC$_{14}$ (25/45/20/10, mol/mol/mol/mol) and 2 mg of ODN in a final solution containing 180 mM citrate, pH 4.0 and 40% ethanol (v/v). All subsequent references to the mol% of specific lipid components of the formu-lation are made with respect to total lipid molar ratios. Encapsulation efficiencies were calculated as the ratio of the initial and final ODN to lipid ratios, multiplied by 100. This was done to minimize the impact of mechanical losses on the absolute recovery of ODN and lipid in small sample sizes. In larger volume formulations, mechanical losses were negli-gible and encapsulation efficiencies were comparable to absolute ODN recoveries.

2.4. HPLC analysis of lipids

Lipid concentrations and mol ratios were deter-mined by HPLC on a Beckman System Gold 128 apparatus equipped with an evaporative light scatter-ing detector (SEDEX 55). Separations were per-formed on a 2.0 mm×150 mm, 5 μm Ultrasphere

cyanopropyl column (Beckman Instruments). The mobile phase consisted of solvent A (99.8% chloroform and 0.2% trifluoroacetic acid) and solvent B (90% isopropyl alcohol, 9.8% distilled water and 0.2% trifluoroacetic acid), filtered through a 0.5 μm filter. Aliquots ($\sim$300 μg total lipid) of lipid formulations were extracted in HBS/chloroform/methanol (1:1:0.3, v/v/v). Individual lipid standards (50–500 μg) were prepared in chloroform to a final volume of 1.0 ml and extracted in HBS (1.0 ml) as described above. The organic phase was analyzed and linear standard curves were generated for each lipid component in the formulation. Extraction recoveries were greater than 95% for all lipid components. Accuracy bias was less than 5%.

2.5. Nuclease protection assays

Free or encapsulated ODN was incubated at 55°C with excess fungal S1 nuclease (100 U nuclease/μg ODN) according to the manufacturer's instructions (Gibco-BRL). In some instances, samples were incubated with Triton X-100 (1% final concentration) to solubilize the lipid vesicles. At various times, aliquots were removed, placed in proteinase K buffer (10 mM Tris, pH 8.0, 100 mM NaCl, 25 mM EDTA, 0.5% SDS and 1 mg/ml proteinase K) and incubated at 50°C for 1 h. Samples were added to an equal volume of stop buffer (93.6% formamide, 20 mM EDTA, 0.05% bromophenol blue) and analyzed on a denaturing 20% PAGE gel containing 7 M urea. Visualization was facilitated using SYBR Green I nucleic acid gel stain (Molecular Probes).

2.6. ^{31}P nuclear magnetic resonance (NMR) spectroscopy

^{31}P NMR spectra were obtained by employing a Bruker MSL200 spectrometer operating at 81 MHz. Free induction decays (FIDs) corresponding to 800 scans were obtained by using a 2.8 μs 50° pulse with a 3 s interpulse delay and a spectral width of 20 000 Hz on a 2.0 ml sample in a 10 mm probe. No proton decoupling was used. An exponential multiplication corresponding to 25 Hz of line-broadening was applied to the FIDs prior to Fourier transformation. The chemical shift is referenced to external 85% phosphoric acid (H_3PO_4). In some instances,

ammonium acetate (150 mM) was added to the exterior of SALP and the pH was adjusted to 7.4 with NaOH. Ammonium acetate equilibrates the interior and exterior pH of the vesicles. In designated spectra, 5 mM $MnSO_4$ was added to the exterior of the vesicles as a membrane impermeable paramagnetic line-broadening agent that quenches the signals of all accessible phosphate groups, including phospholipids and ODN.

2.7. Cryo-electron microscopy

A single drop of buffer containing SALP was applied to a standard electron microscopy grid with a perforated carbon film. Excess liquid was removed by blotting, leaving a thin layer of the suspension covering the holes of the carbon film. The grid was rapidly frozen in liquid ethane, resulting in vesicles embedded in a thin film of amorphous ice. Images of the vesicles in the ice were obtained under cryogenic conditions at a magnification of 50 000 and a defocus of -1.5 microns using a Gatan cryo-holder in a Philips CM200 FEG electron microscope.

2.8. Mice

Female, ICR mice (7–9 weeks) were purchased from Harlan-Sprague Dawley (Indianapolis, IN, USA) and were quarantined for 1 week prior to use. All studies were conducted in accordance with the guidelines established by the Canadian Council on Animal Care (CCAC).

2.9. Plasma clearance of SALP

For pharmacokinetic studies, SALP formulations containing PS ODN labeled by incorporation of a [^3H]thymidine base or ^{35}S label in the PS backbone were concentrated to approximately 12.5 mg/ml total lipid using a hand-held diafiltration apparatus (A/G Technology Corp., Needham, MA, USA) attached to 10 cc syringes. Samples of free or encapsulated [^3H]ODN were administered i.v. via the lateral tail vein of ICR mice at a dosing volume of 10 ml/kg. Lipid and ODN doses were 100 and 15 mg/kg body weight (unless otherwise indicated), representing an ODN to lipid ratio of 0.15, weight of ODN/weight of total lipid. At various times, mice were anesthetized

with ketamine/xylazene, and blood was collected by cardiac puncture prior to euthanasia. Plasma was collected and analyzed for radioactivity using standard liquid scintillation techniques. No significant differences in the circulation profiles were observed over 24 h using the different radiolabels.

3. Results

3.1. Encapsulation of PS ODN in SALP

It is relatively straightforward to passively encapsulate anionic antisense ODN in the aqueous space of conventional lipid vesicles [20,21,34]. However, to achieve even modest encapsulation efficiencies of 5–10% in a population of large unilamellar vesicles (LUV) with a mean diameter of 100 nm, extreme concentrations of lipid and ODN must be employed. This makes formulation difficult, time consuming and wasteful. The inclusion of 1–20 mol% cationic lipid improves the association of anionic ODN and plasmid DNA with vesicles through electrostatic interactions, but when these systems are administered i.v. they are rapidly eliminated from the circulation [22–24,35] and exhibit poor accumulation at disease sites, such as tumors and sites of inflammation [36,37]. Consequently, it was determined that ionizable cationic lipids might be a better choice in that formulations could be made at acidic pH, when the majority of the lipid was cationic, but the resulting delivery system would be charge 'neutral' when administered at physiological pH.

DODAP was employed as an ionizable cationic lipid as it exhibits an apparent pK of 6.6 in lipid bilayer systems [38]. Encapsulation relying on electrostatic interactions between ODN and cationic lipid can therefore occur at acidic pH values (i.e. pH 4.0), whereas subsequent adjustment of the external pH to neutral pH values should result in a neutral surface charge on the resulting particles. In order to minimize aggregation and fusion between particles during the formulation process, PEG-CerC$_{14}$, a steric barrier lipid, was included in the formulation. Initial studies were conducted using a lipid mixture of DSPC, CH, DODAP and PEG-CerC$_{14}$ (25/45/20/10, mol/mol/mol/mol). A dried lipid film was hydrated with an aqueous solution of PS ODN in

300 mM citrate buffer, pH 4.0, and the resulting liposomes sized to 100 nm diameter vesicles by extrusion at 65°C. The external buffer was exchanged for buffered saline (pH 7.6) to neutralize the positive charge due to DODAP. The vesicles were subsequently passed through an ion-exchange column to remove residual ODN. This process yielded an encapsulation efficiency of approximately 30%. However, the extrusion process was slow and as much as 30% of both the starting lipid and antisense ODN was lost because of the formation of ODN/lipid aggregates that were trapped on the filters.

3.2. Influence of ethanol on encapsulation of ODN

In an effort to improve the encapsulation efficiency and reduce losses during extrusion, ethanol was
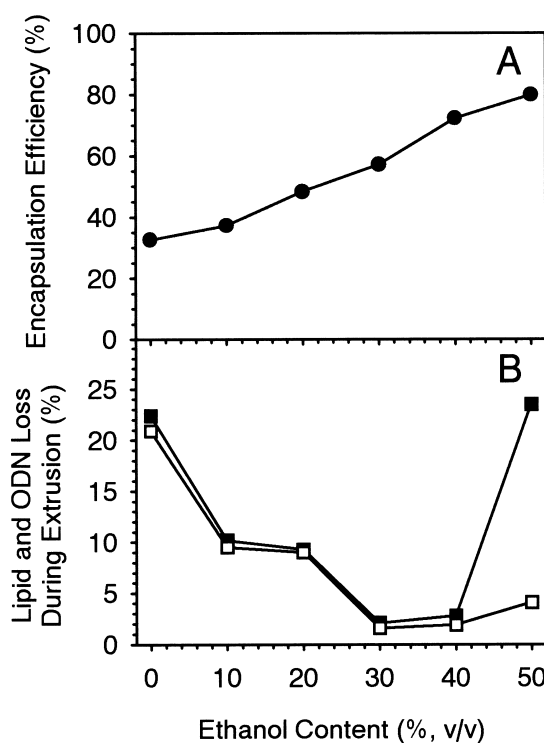

Fig. 1. Influence of ethanol on final encapsulation efficiency (A) and sample recoveries during extrusion (B) of SALP. Lipid films composed of a 10 mg (total lipid) mixture of DSPC/CH/DODAP/PEG-CerC$_{14}$ (25/45/20/10, mol/mol/mol/mol) were hydrated with 2 mg hICAM ODN in 1.0 ml citrate buffer, pH 4.0 containing varying concentrations of ethanol, as described in Section 2. Lipid (□) and ODN (■) loss during particle size reduction (extrusion) was determined by both radiolabel and HPLC analysis and gave comparable results.

added to the ODN solution used to rehydrate the lipid films. As lipid vesicles are able to form even in relatively high concentrations of ethanol [39], we speculated that the presence of this solvent might increase the deformability of the DNA/lipid particles; thereby, facilitating the self-assembly and size reduction processes. In the presence of increasing concentrations of ethanol, the encapsulation efficiency increased in a near-linear manner (Fig. 1A). Residual alcohol was readily removed by dialysis. Optimal processing occurred at 40% ethanol, with rapid extrusion times and minimal losses of lipids and ODN ($<3\%$) during size reduction (Fig. 1B). At higher ethanol concentrations ($>50\%$), significant and visible aggregation and precipitation was observed. At this ethanol concentration, some ODN was lost through precipitation very early in the formulation process (Fig. 1B); however, no additional losses of ODN were observed following dialysis and anion-exchange chromatography, indicating complete encapsulation of the residual ODN. At lower ethanol concentrations, the particles were less deformable and more ODN adsorbed to the surface of the vesicles and was subsequently lost following charge neutralization of the DODAP, dialysis and anion-exchange chromatography. Given the positive impact of ethanol on the ease of formulation and sample recovery, the process was subsequently further simplified in that the requisite lipid mixture was dissolved in 100% ethanol and added to ODN dissolved in citrate buffer, pH 4.0 (2/3, v/v, ethanol/citrate). This modification eliminated the requirement for lipid films and greatly reduced sample processing times.

In the absence of a steric barrier lipid, extensive aggregation and fusion was observed upon addition of the cationic lipid mixture to ODN at final ethanol concentrations $>20\%$ (v/v). The addition of PEG-CerC$_{14}$ lipid to the formulation at 10 mol% (with respect to total lipid) eliminated this phenomenon, consistent with the known role of PEG-lipid in preventing the aggregation and fusion between lipid vesicles [40]. An examination of the minimum quantity of PEG-lipid required to form stable particles indicated that wholesale aggregation and fusion was prevented at $\geq 5\%$ PEG-lipid. Given the relatively short chain length of the PEG-CerC$_{14}$ hydrophobic anchor, there was the possibility that some

PEG-lipid may be lost during prolonged dialysis through the dissociation of PEG-lipid monomers from the vesicle membrane. To evaluate this and to monitor the fate of the formulation components during the preparation process, HPLC analyses were performed at various stages during the formulation process.

In a typical formulation consisting of DSPC/CH/DODAP/PEG-CerC$_{14}$ at a theoretical initial lipid concentration of 10 mg/ml (total lipid), individual lipid concentrations were determined to be 2.40, 4.97, 2.61 and 1.12 mg/ml, respectively (11.1 mg/ml total lipid; 150 ml formulation volume). In the final preparation following dialysis and concentration, these lipid concentrations were observed to be 3.68, 7.33, 4.14 and 1.74 mg/ml, respectively (16.9 mg/ml total lipid; 91 ml final volume), indicating that very little loss of lipid components occurs during the formulation process. Total lipid recovery was 92.4%. However, sucrose density gradient isolation of SALP prepared at high ODN to lipid ratios and containing [^{14}C]CHE and [^{3}H]PEG-CerC$_{14}$ markers indicated that >60–70% of the initial PEG-lipid was excluded from the final vesicles and probably exists
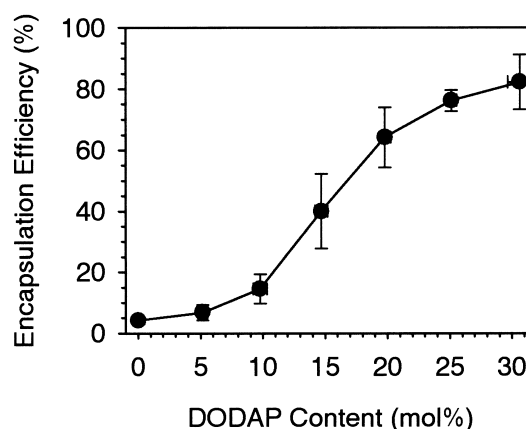

Fig. 2. Influence of aminolipid (DODAP) content on encapsulation of ODN in SALP. SALP were prepared by the addition of an ethanol solution containing lipid to hICAM ODN in citrate buffer, pH 4.0, as described in Section 2. The mol% DODAP was varied at the expense of DSPC. The CH and PEG-CerC$_{14}$ contents were held constant at 45 mol% and 10 mol%, respectively. The indicated mol% are with respect to all (total) lipid components. The actual DODAP content (mol%) in each sample was determined by HPLC analysis as described in Section 2. The data points represent the mean ± S.D. of four experiments.

as PEG-lipid micelles, since no PEG-lipid was lost during the dialysis step.

3.3. Influence of DODAP on encapsulation efficiency

The optimal DODAP concentration for formulation was determined in DSPC/CH/DODAP/PEG-CerC$_{14}$ vesicles in the presence of 40% ethanol, 2 mg/ml ODN and 10 mg/ml total lipid. The mol% DODAP in the formulation was varied at the expense of DSPC. As shown in Fig. 2, encapsulation efficiency increased from 5 to 80% as the concentration of DODAP was increased from 0 to 30 mol%. In formulations with DODAP concentrations greater than 30 mol%, vesicle size reduction became more difficult. This phenomenon was not observed in the absence of ODN and was therefore most likely a consequence of enhanced DODAP/ODN interactions that resulted in an increased charge ratio ($\pm$) and the formation of larger particles. Consequently, 20–25 mol% DODAP was considered to be an optimal concentration for further characterization. The influence of pH on ODN encapsulation was evaluated employing a lipid composition consisting of DSPC/CH/DODAP/PEG-CerC$_{14}$ (25/45/20/10), 40% ethanol in citrate buffer, 2 mg/ml ODN and 10 mg/ml total lipid. The encapsulation efficiency increased from 5 to >90% as the pH was decreased through
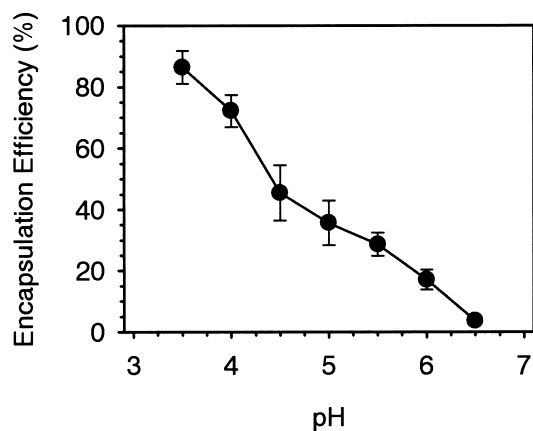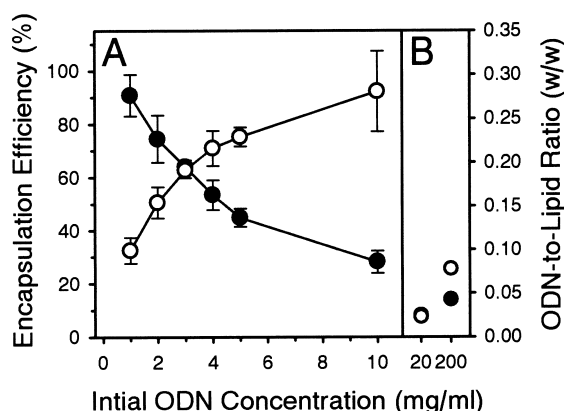

Fig. 4. Optimization of ODN to lipid ratios in SALP (A) and by passive encapsulation in EPC:CH liposomes (B). ODN was encapsulated in DSPC/CH/DODAP/PEG-CerC$_{14}$ (20/45/25/10, mol/mol/mol/mol) vesicles upon addition of an ethanol solution containing lipid to varying concentrations of hICAM ODN in citrate buffer containing 40% ethanol, as described in Section 2. Alternatively, ODN was entrapped in 100 nm EPC/CH (55/45, mol/mol) liposomes by passive encapsulation techniques. The lipid concentrations in these instances were 50 mg/ml (20 mg/ml ODN) and 250 mg/ml (200 mg/ml ODN). The encapsulation efficiency (●) and resulting ODN to lipid ratios (○) are indicated. The data points represent the mean ± S.D. of three experiments.

the pK range of DODAP, pH 7 to pH 4 (Fig. 3). Under the conditions employed in this study (180 mM citrate buffer, pH 4.0 and 25 mol% DODAP), the apparent pK_a of DODAP was determined to be 5.8 by measuring the bulk proton concentration in the absence of ethanol as outlined in Bailey et al. [38]. These results highlight the importance of electrostatic interactions in the formulation process and indicate that at physiological pH the formulation would have little residual surface charge.

One concern in formulating ODN at acidic pHs was the potential loss of purine bases through hydrolysis. PS ODN was therefore incubated at pH 4 and 65°C and analyzed by mass spectrometry and HPLC. The levels of depuration detected following a 2 h incubation were less than 3%. A typical laboratory scale formulation can be prepared in less than 30 min with undetectable levels of degradation. For larger scale formulations where processing times may increase to several hours, solutions are only raised to 65°C when necessary, thereby limiting depuration to <0.5%. After encapsulation of ODN and adjustment of the external pH to 7.6, the transmembrane

Fig. 3. pH Dependence of ODN encapsulation in SALP. ODN was encapsulated in DSPC/CH/DODAP/PEG-CerC$_{14}$ (20/45/25/10, mol/mol/mol/mol) vesicles upon addition of an ethanol solution containing lipid to hICAM ODN in citrate buffer, as described in Section 2. The measured pH of the buffer in the absence of ethanol, ODN and lipid is indicated (●). The data points represent the mean ± S.D. of three experiments.

pH gradient, measured by the distribution of methylamine [41], indicated an internal pH of 5.5–6.0.

3.4. Optimization of ODN to lipid ratios

At a constant lipid concentration of 10 mg/ml total lipid, the final ODN to lipid ratio was varied from 0.08 to 0.25 (w/w) by increasing the initial ODN concentrations from 1 to 10 mg/ml (Fig. 4A). As the final ODN to lipid ratio increased, a concomitant decrease in the encapsulation efficiency from 90–95% to 25–30% was observed. Through this range, the ODN to lipid ratio increased from 0.1 to 0.25. Standardized conditions for ODN encapsulation (2.0–2.5 mg/ml ODN and 10 mg/ml total lipid) were chosen that typically yield 65–75% encapsulation with an ODN to lipid ratio of 0.15–0.20 (w/w). In comparison, under the same conditions of lipid and antisense concentration, the hydration of a dry lipid film composed of EPC:CH would yield an encapsulation efficiency of approximately 3% and an ODN to lipid ratio of 0.002 [21]. Increasing the lipid concentration (50 and 250 mg/ml) in this EPC:CH system resulted in modest increases in encapsulation efficiencies and ODN to lipid ratios, but even at the highest lipid concentration the resulting encapsulation efficiency and ODN to lipid ratios were only 14% and 0.08, respectively (Fig. 4B).

The DODAP formulation process appears to be independent of ODN sequence, has been tested for PS ODN varying in length from 15 to 24 bases and is applicable to phosphodiester ODN, synthetic ribozymes, and plasmid DNA (Maurer et al., manuscript in preparation). We refer to the ODN-loaded vesicles produced by this procedure as SALP.

3.5. Protection of ODN from nuclease degradation

It is important to demonstrate that the ODN in SALP is indeed encapsulated within the lipid vesicles and not simply adsorbed to the vesicle surface. To demonstrate protection from extracellular nucleases, aliquots of free and encapsulated ODN were incubated with excess fungal S1 nuclease for various times, in the presence or absence of Triton X-100. Free PS ODN was completely degraded in less than 5 min while no detectable degradation was observed for up to 24 h for the encapsulated ODN (Fig. 5). This protection was lost following the addition of detergent to solubilize the lipid bilayer, strongly suggesting that the ODN was encapsulated.

3.6. Evaluation of ODN encapsulation by ^{31}P NMR

Since SALP contain a PEG surface coating that may sterically shield the surface of vesicles from nuclease activity, ^{31}P NMR was used to confirm that the ODN was encapsulated in the interior of the
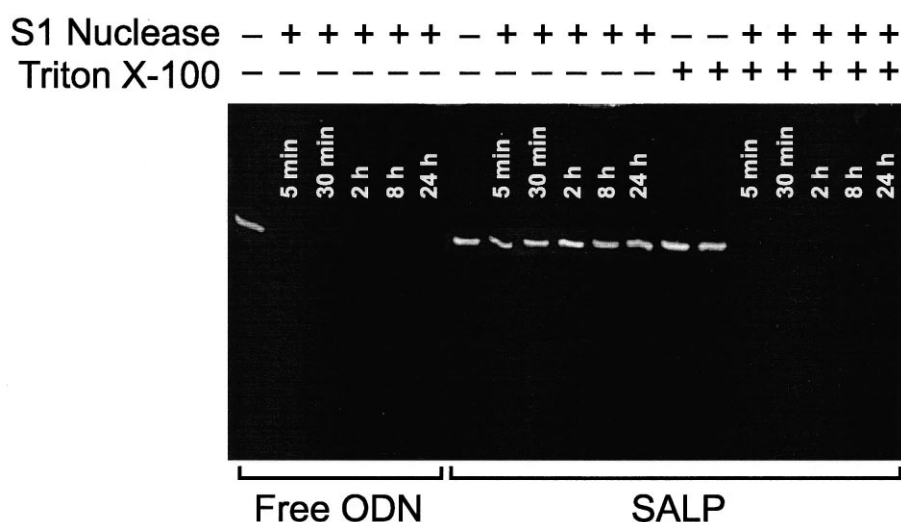

Fig. 5. Nuclease protection of ODN. Encapsulation and protection of ODN was initially demonstrated using a nuclease protection assay. Free ODN or SALP were incubated with 100 U of S1 nuclease in the presence or absence of 1% Triton X-100. At the indicated times, aliquots of the incubation mixture were removed and analyzed for ODN integrity as outlined in Section 2.

vesicles. All of the spectra shown were obtained from samples containing the same concentration of c-myc ODN (2.0 mg/ml) (Fig. 6). When c-myc ODN was free in solution, a sharp ^{31}P NMR signal was detected (spectrum 1), however, the signal from the same concentration of c-myc ODN encapsulated in SALP (spectrum 2) was broadened beyond detection under the spectrometer conditions employed (see Section 2). These data can be explained if the entrapped ODN is bound to the interior membrane surface through electrostatic interactions with the cationic form of DODAP, and therefore immobilized on the NMR time-scale. The aqueous core of the SALP is pH 5.5–6.0, a range in which a large proportion of DODAP molecules will be positively charged. When this transmembrane pH gradient is collapsed and equilibrated to pH 7.4 by the addition of 150 mM ammonium acetate and NaOH to the external buffer, a ^{31}P NMR signal for the ODN became apparent (spectrum 3). This is consistent with the neutralization of DODAP and subsequent release of ODN from the membrane surface and into solu-
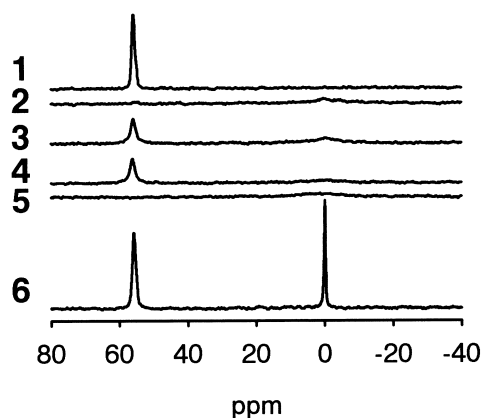

Fig. 6. ^{31}P NMR determination of ODN encapsulation. Encapsulation of PS c-myc ODN was assessed using a ^{31}P NMR assay as described in Section 2 and in the text. The individual spectra represent: (1) free ODN in HBS, pH 7.4; (2) ODN encapsulated in SALP exhibiting interior pH ∼ 5.5/exterior pH 7.4; (3) sample 2 with the interior pH raised to 7.4 using 150 mM ammonium acetate; (4) sample 3 with 5 mM MnSO$_4$ added to the exterior of SALP; (5) sample 4 with 200 mM octyl-β-D-glucopyranoside (OGP) added to solubilize SALP; and (6) SALP solubilized by 200 mM OGP. All samples contained 2.0 mg/ml ODN. All spectral intensities corresponding to 800 scans were normalized to 2.0 mg/ml antisense. Integrated signal intensities (± 0.05 mg/ml) in mg/ml are: 2.00 (1); 0.00 (2); 1.24 (3); 1.24 (4); 0.00 (5); 2.00 (6). T_1 values, 1.7 s (1); 2.1 s (3). Chemical shifts are referenced to external 85% H$_3$PO$_4$.

tion where its motion can be detected. The final three spectra demonstrate that the signal shown in spectrum 3 arises from c-myc PS ODN encapsulated inside the SALP. The addition of 5 mM MnSO$_4$, a membrane impermeable NMR line-broadening reagent, had no effect on the signal intensity until the sample was solubilized in 200 mM OGP, after which the ^{31}P signal was eliminated (spectra 4 and 5, respectively). However, in the absence of MnSO$_4$, solubilization in detergent at pH 7.4 produced two sharp ^{31}P NMR signals, one from c-myc PS ODN free in solution and the other arising from phospholipids in detergent micelles (spectrum 6).

The ^{31}P NMR signal intensities for ODN shown in spectra 1 and 6 were the same, however, the signal from the same concentration of encapsulated ODN was attenuated by about 40% (spectra 3 and 4). This was not due to NMR resonance saturation because the spin-lattice relaxation times (T_1) of free ($T_1 =$ 1.7 s) and encapsulated ($T_1 = 2.1$ s) ODN at pH 7.4 were essentially the same. The T_1 values were measured by an inversion-recovery pulse sequence on samples 1 and 3. Furthermore, the interpulse delay of 3 s for 50° pulses allows for complete relaxation of all ODN resonances. The attenuation of signal intensity shown in spectra 3 and 4 can be attributed to several possibilities, including incomplete solubility of the encapsulated ODN in the aqueous core of the particle, or the existence of secondary ODN-lipid structures within SALP.

3.7. Evaluation of SALP by cryo-electron microscopy

Freeze-fracture electron microscopy and quasielastic light scattering (QELS) indicated that SALP were composed of a homogeneous population of vesicles with a mean diameter of 110 ± 30 nm. The vesicle size distribution was stable for at least 6 months during storage at 4°C. To investigate the potential existence of secondary structures within SALP, a cryo-electron microscopy analysis of SALP was performed at two different ODN to lipid ratios (0.025 and 0.25, w/w) and revealed several interesting structural features (Fig. 7). At the higher ODN to lipid ratio, the SALP preparation consisted of spherical vesicles, with populations of LUV and small multilamellar vesicles (SMLV) (Fig. 7, bottom panel). The average particle sizes were the same as
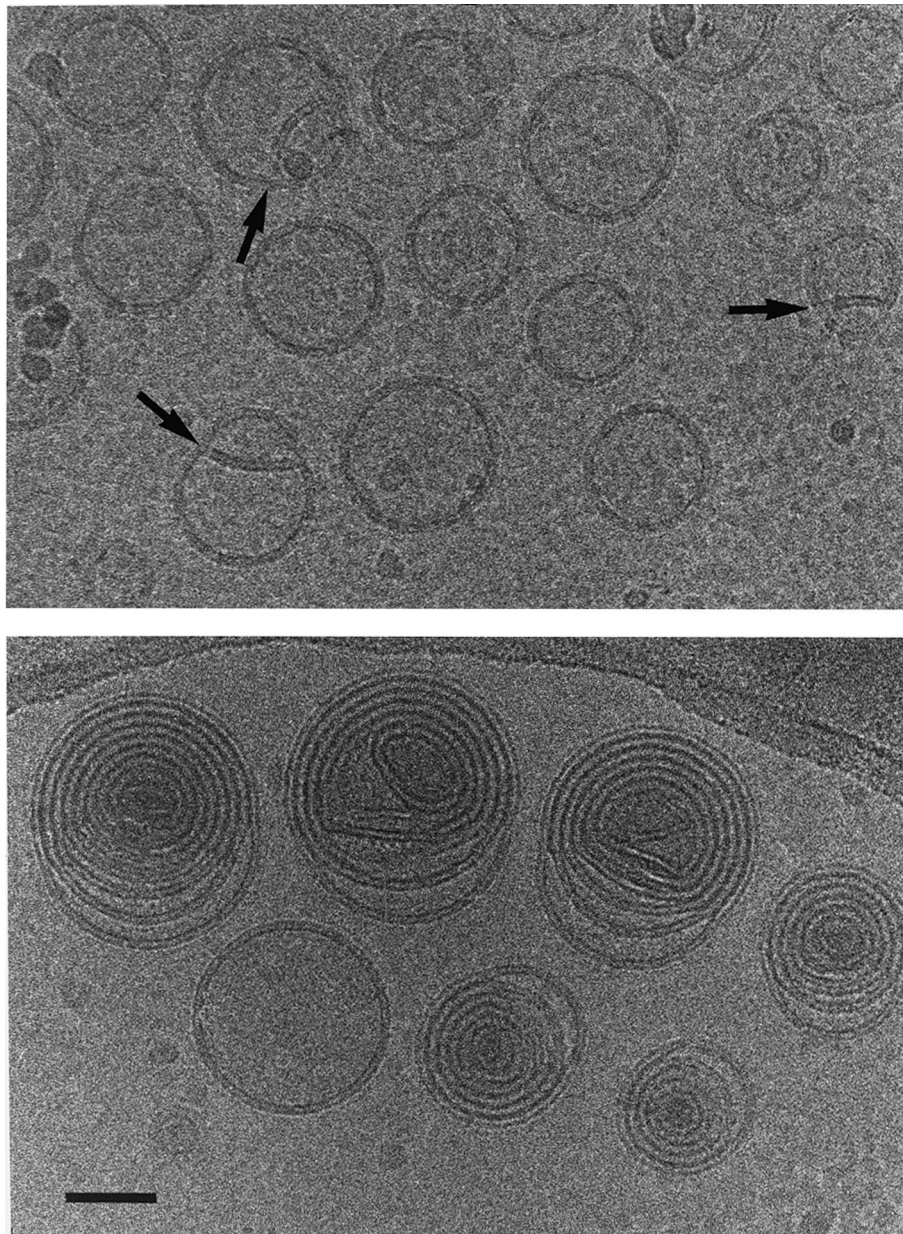
Fig. 7. Cryo-electron microscopy of SALP. The structure of SALP was evaluated at low (top panel) and high (bottom panel) initial ODN to lipid ratios (0.025, w/w and 0.25, w/w, respectively). Magnification in each panel was 50 000×. The scale is represented by the bar (50 nm).

determined previously by freeze-fracture and QELS analyses. The SMLV consisted of numerous lamellae (typically 6–9) arranged as concentric rings inside the particle core such that the innermost structures exhibit diameters as small as 20 nm (Fig. 7, bottom panel). In general the encapsulated membrane structures are closely associated; however, many of the particles share a common feature where the outer 2–4 lamellae at one side of the particle appear to separate (Fig. 7, bottom panel). Interestingly, at the low ODN to lipid ratio SALP are predominantly unilamellar, but most exhibit a cap-like structure (Fig. 7, top panel, arrow) that may represent the interaction between two vesicles and could be a pre-cursor to the SMLV structures observed at higher ODN to lipid ratios. The SMLV structures of
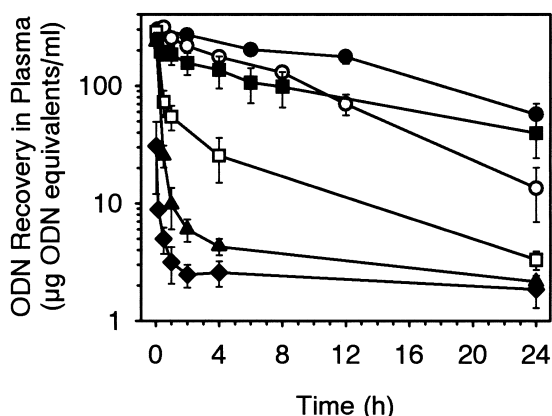
Fig. 8. Circulation profiles in mice. The influence of surface charge and presence of a steric polymer surface coating on the circulation of SALP was evaluated upon i.v. administration in ICR mice. Formulations contained ^{3}H-labeled mICAM ODN and were administered at ODN doses of 15 mg/kg and approximate lipid doses of 100 mg/kg body weight. Formulations evaluated were: DSPC/CH/DODAP/PEG-CerC$_{20}$ (●), DSPC/CH/DODAP/PEG-CerC$_{14}$ (○), DSPC/CH/DODAC/PEG-CerC$_{20}$ (■), DSPC/CH/DODAC/PEG-CerC$_{14}$ (□), DODAC/dioleoylphosphatidylethanolamine (DOPE) (1/1)/ODN complexes (◆), and free ODN (▲). Except where indicated, the lipid ratios were 20/45/25/10 (mol/mol/mol/mol). The data points represent the mean ± S.D. from five animals.

SALP observed in Fig. 7 suggest a constrained mobility of antisense between the lipid bilayers, possibly explaining the reduced NMR signal described above.

3.8. Pharmacokinetics of SALP

The plasma circulation profile of SALP, containing a [^{3}H]thymidine labeled ODN, was monitored in ICR mice after i.v. administration at a dose of approximately 100 mg lipid/kg body weight (15 mg ODN/kg body weight). To highlight the importance of the aminolipid on the circulation times, SALP formulations containing ionizable and quaternary aminolipids were investigated. In addition, these formulations contained either PEG-CerC$_{14}$ or PEG-CerC$_{20}$. The PEG-CerC$_{14}$ lipid is able to rapidly diffuse out of the lipid bilayer, with an in vitro half-life of ∼1.1 h [42]. Under the same conditions, the exchange rate of the PEG-CerC$_{20}$ is much slower (∼13 days), and this lipid is therefore able to provide steric protection against interaction with plasma proteins and allow extended circulation times com-

parable to classical sterically stabilized liposomes containing PEG$_{2000}$-DSPE [28,43].

SALP containing DODAP and either PEG-CerC$_{14}$ or PEG-CerC$_{20}$ exhibited monophasic plasma elimination profiles and half-lives ($t_{1/2}$ ∼ 5–6 h and 10–12 h, respectively) that were significantly longer than the circulation half-life of free PS ODN ($t_{1/2}$ 5–10 min) (Fig. 8). In contrast, when SALP contained a quaternary aminolipid (DODAC), the plasma elimination profiles were much more rapid. Formulations containing DODAC and either PEG-CerC$_{14}$ or PEG-CerC$_{20}$ exhibited half-lives of approximately 15 min and 2–3 h, respectively. This difference likely reflects the ability of PEG-CerC$_{20}$ to inhibit the interactions between the predominantly anionic plasma proteins and the cationic lipid vesicles, thereby reducing opsonization and increasing the plasma residence time of the formulation [43]. Rapid plasma elimination ($t_{1/2} < 5$ min) was also observed for DOPE/DODAC (1/1)/ODN lipoplexes administered at lipid doses comparable to the SALP formulations.

4. Discussion

Effective, systemic delivery systems for DNA and RNA are considered basic to the successful clinical application of gene-based drugs [4,44–46]. In this study, we describe and characterize a novel lipid-based formulation (SALP) designed for i.v. delivery of polyanionic oligonucleotides. The formulation process represents a significant improvement over existing methods as ODN are encapsulated with both high efficiency and high drug to lipid ratios, while employing simple manufacturing techniques.

Other lipid mixtures and encapsulation protocols have been applied to oligonucleotides with varying degrees of success. Standard methods, employing net neutral lipid mixtures, yield low encapsulation efficiencies and drug to lipid ratios (reviewed in [20,21]). This can be overcome by incorporating cationic lipids into the formulation, but the resulting lipid/nucleic acid complexes are typically unstable and exhibit limited circulation times [22–24]. For example, Gokhale et al. have recently described a liposomal formulation composed of PC/CH/DDAB (55/28/17, mol/mol/mol) and raf-1 ODN that sensitizes radioresistant SQ-20B xenografted tumors to ioniz-

ing radiation [23]. However, only ∼1% of the total administered dose remained in the circulation at 5 min post-administration. Moreover, in this type of system, significant quantities of oligonucleotide would be expected to remain associated with the positively charged surface of the particles and dissociate from the carriers in the blood. The MVE approach employed by Thierry et al. [47,48] generates high encapsulation efficiencies (comparable to SALP) and drug to lipid ratios (approximately 2–4-fold lower than SALP). However, the formulation employs 3–7 mol% cardiolipin (CL), a potent activator of rat and human complement [25,26]. Furthermore, similar liposome formulations (EPC/CH/CL, 45/45/10) containing CL have been shown to exhibit very short circulation times, therefore the clinical application of this formulation would be expected to be limited [49]. Another approach to improving encapsulation has been to chemically modify oligonucleotides, making them more lipophilic [44,50]. However, these molecules are insoluble in aqueous environments which, until recently, has limited their clinical development [51].

While nuclease protection assays and ^{31}P NMR studies indicate that ODN is encapsulated within SALP, the mechanism of SALP formation and ODN entrapment is not fully understood. In this regard, Huebner et al. recently observed the formation of compact multilamellar structures when fragmented, linear genomic DNA (average 6000 bp) was added to unilamellar cationic vesicles composed of DMPC/DC-Chol (3:2, molar ratio) [52]. Employing cryo-electron microscopy, these authors showed structures that resemble the tightly associated, concentric bilayers presented in Fig. 7 (bottom panel). To explain their results, they present a model in which vesicles, coated with an adsorbed layer of DNA, are forced into close contact with neighboring vesicles through electrostatic interactions. The vesicles become flattened and deformed in the contact region with DNA sandwiched between the membranes. Changes in lipid packing resulting from lateral separation of lipids and a reduction of headgroup area induced by the charge neutralization of DC-Chol by DNA are proposed as two factors that contribute to the destabilization of vesicles causing them to fuse and/or rupture. Sequential binding, flattening and rupture of vesicles are presented as a mechanism for the formation of the highly compact multilamellar structures.

Although there are significant differences between the DNA/lipid structures described by Huebner et al. [52] and SALP, the mechanism by which the two form may be related. Spontaneous formation of small unilamellar vesicles is expected to occur upon rapid dilution of the ethanol-lipid solution in aqueous buffer [53]. The negatively charged ODN will interact with the cationic vesicles and lateral separation of the cationic form of DODAP, facilitated by high ethanol concentration, could lead to the formation of membrane patches enriched with DODAP and depleted of PEG. This hypothesis is supported by the observation that >60–70% of the initial PEG-lipid was excluded from the final vesicles. Therefore, the distended bilayers observed in each of the SMLVs may reflect areas in which PEG-lipids have concentrated due to lateral separation effects (Fig. 7). The structural features of SALP and the mechanisms of formation are currently under further investigation.

It is interesting to note that for SALP containing 25 mol% DODAP, an ODN to lipid ratio (w/w) of 0.1 is sufficient for complete charge neutralization, assuming all the cationic lipid is ionized and each ODN base carries a net negative charge at the loading pH. Therefore, to achieve ratios greater than this suggests that the electrostatic interaction between DODAP and the ODN bases is not stoichiometric under the formulation conditions. At pH 4.0 it is expected that >99% of the DODAP molecules will carry a positive charge. However, the net negative charge on the ODN may be less than expected, based on the number of bases, when the pK values of the phosphates (pK 3–3.5) and protonation of bases such as cytosine (pK ∼4.6) are taken into consideration. Therefore, a reduction in net negative charge per ODN molecule may account for the loading stoichiometry observed for SALP with ODN to lipid ratios (w/w) >0.1.

The ionizable lipid and the PEG-Cer molecules used to construct SALP endow this system with unique features. The ionizable cationic lipid DODAP facilitates efficient charge-dependent loading at acidic pH values, but also allows SALP to exhibit a near-neutral surface charge at physiological pH. As a result, SALP can achieve extended circulation lifetimes

following i.v. administration and would be expected to exhibit preferential accumulation at disease sites such as tumors and sites of inflammation [54,55]. In addition, the neutral form of DODAP has been shown to induce fusion in model membrane systems [38] and consequently may promote fusion on interaction of SALP with cell membranes, thereby enhancing intracellular delivery of ODN. However, there is no direct evidence at this time that this actually occurs. With regard to the PEG-CerC$_{14}$ or PEG-CerC$_{20}$ constituents, which are required to stabilize SALP during formulation, it should be noted that PEG coatings inhibit vesicle–vesicle and vesicle–membrane association and fusion [40], and thus would be expected to inhibit intracellular delivery of ODN after reaching the disease site. However, the PEG-CerC$_{14}$ species exhibits a half-time for dissociation from lipid vesicles in vivo of 3–6 min (Semple et al., manuscript submitted) following i.v. administration and therefore would not be associated with SALP when the particles reached a disease site. Recently, Stuart et al. have demonstrated that lipid/ODN particles prepared by a reverse-phase technique, in which the cationic lipid becomes sequestered in the inner monlayer of the vesicles during preparation thereby minimizing external surface charge, had long circulation times in vivo and reduced the expression of P-glycoprotein in multidrug-resistant human B-lymphoma cells in vitro [56,57]. These results confirm that the general strategy of reducing surface charge in lipid-based formulations of ODN is practical and may be important in the development of clinically viable systemic in vivo delivery systems for antisense ODN.

In summary, we believe SALP represent a safe and practical means to radically alter the pharmacokinetic characteristics of anionic antisense drugs and overcome many of the drawbacks associated with the clinical development of PS ODN and lipid-based formulations thereof. As such, we are currently investigating the biochemical and pharmacological activity of SALP formulations containing ODN specific for anti-inflammatory (ICAM-1) and oncology-based (c-myc and c-myb proto-oncogenes) targets. Studies thus far indicate that SALP containing entrapped ODN potentiate a range of desirable biological effects in vivo; including both antisense-specific and non-specific effects (enhanced activation of NK cells, monocytes/macrophages and cytokines). Moreover, we believe that this type of delivery system will be broadly applicable to other DNA- and RNA-based therapeutic agents and that, by choosing an appropriate ionizable lipid, it will be possible to encapsulate a wide variety of charged compounds, including proteins, peptides, and other diagnostic and therapeutic agents. Finally, the unique SMLV structures observed in this study provide further insight into the interactions of DNA with cationic lipids and lipid membranes and may aid in the design of more effective delivery systems for nucleic acid therapeutics.

References

[1] D.M. Prazeres, G.N. Ferreira, G.A. Monteiro, C.L. Cooney, J.M. Cabral, Large-scale production of pharmaceutical-grade plasmid DNA for gene therapy: problems and bottlenecks, Trends Biotechnol. 17 (1999) 169–174.

[2] S. Akhtar, R. Kole, R.L. Juliano, Stability of antisense DNA oligodeoxynucleotide analogs in cellular extracts and sera, Life Sci. 49 (1991) 1793–1801.

[3] M.J. Hope, B. Mui, S. Ansell, Q.F. Ahkong, Cationic lipids, phosphatidylethanolamine and the intracellular delivery of polymeric, nucleic acid-based drugs, Mol. Membr. Biol. 15 (1998) 1–14.

[4] Y. Rojanasakul, Antisense oligonucleotide therapeutics: drug delivery and targeting, Adv. Drug Deliv. Rev. 118 (1996) 115–131.

[5] S. Agrawal, R. Zhang, Pharmacokinetics of oligonucleotides, Ciba Found. Symp. 209 (1997) 60–75.

[6] S.T. Crooke, M.J. Graham, J.E. Zuckerman, D. Brooks, B.S. Conklin, L.L. Cummins, M.J. Greig, C.J. Guinosso, D. Kornbrust, M. Manoharan, H.M. Sasmor, T. Schleich, K.L. Tivel, R.H. Griffey, Pharmacokinetic properties of several novel oligonucleotide analogs in mice, J. Pharmacol. Exp. Ther. 277 (1996) 923–937.

[7] S.P. Henry, P.C. Giclas, J. Leeds, M. Pangburn, C. Auletta, A.A. Levin, D.J. Kornbrust, Activation of the alternative pathway of complement by a phosphorothioate oligonucleo-

tide: potential mechanism of action, J. Pharmacol. Exp. Ther. 281 (1997) 810–816.

[8] S.P. Henry, W. Novotny, J. Leeds, C. Auletta, D.J. Kornbrust, Inhibition of coagulation by a phosphorothioate oligonucleotide, Antisense Nucleic Acid Drug Dev. 7 (1997) 503–510.

[9] W.M. Galbraith, W.C. Hobson, P.C. Giclas, P.J. Schechter, S. Agrawal, Complement activation and hemodynamic changes following intravenous administration of phosphorothioate oligonucleotides in the monkey, Antisense Res. Dev. 4 (1994) 201–206.

[10] E. Uhlmann, A. Peyman, D.W. Will, Antisense: chemical modifications, in: J.R. Bertino (Ed.), Encyclopedia of Cancer, Academic Press, San Diego, CA, 1997, pp. 64–81.

[11] J.T. Holmlund, B.P. Monia, T.J. Kwoh, F.A. Dorr, Toward antisense oligonucleotide therapy for cancer: ISIS compounds in clinical development, Curr. Opin. Mol. Ther. 1 (1999) 372–385.

[12] A. Chonn, P.R. Cullis, Recent advances in liposomal drug-delivery systems, Curr. Opin. Biotechnol. 6 (1995) 698–708.

[13] M.S. Webb, T.O. Harasym, D. Masin, M.B. Bally, L.D. Mayer, Sphingomyelin-cholesterol liposomes significantly enhance the pharmacokinetic and therapeutic properties of vincristine in murine and human tumour models, Br. J. Cancer 72 (1995) 896–904.

[14] L. Embree, K. Gelmon, A. Tolcher, N. Hudon, J. Heggie, C. Dedhar, P. Logan, M.B. Bally, L.D. Mayer, Pharmacokinetic behavior of vincristine sulfate following administration of vincristine sulfate liposome injection, Cancer Chemother. Pharmacol. 41 (1998) 347–352.

[15] L.D. Mayer, L.C. Tai, D.S. Ko, D. Masin, R.S. Ginsberg, P.R. Cullis, M.B. Bally, Influence of vesicle size, lipid composition, and drug-to-lipid ratio on the biological activity of liposomal doxorubicin in mice, Cancer Res. 49 (1989) 5922–5930.

[16] A.S. Janoff, L.T. Boni, M.C. Popescu, S.R. Minchey, P.R. Cullis, T.D. Madden, T. Taraschi, S.M. Gruner, E. Shyamsunder, M.W. Tate, R. Mendelsohn, D. Bonner, Unusual lipid structures selectively reduce the toxicity of amphotericin B, Proc. Natl. Acad. Sci. USA 85 (1988) 6122–6126.

[17] O. Zelphati, F.C. Szoka Jr., Cationic liposomes as an oligonucleotide carrier: Mechanism of action, J. Liposome Res. 7 (1997) 31–49.

[18] N. Smyth-Templeton, D.D. Lasic, P.M. Frederik, H.H. Strey, D.D. Roberts, G.N. Pavlakis, Improved DNA:liposome complexes for increased systemic delivery and gene expression, Nat. Biotechnol. 15 (1997) 647–652.

[19] A.R. Thierry, G.B. Takle, Liposomes as a delivery system for antisense and ribozyme compounds, in: S. Akhtar (Ed.), Delivery Strategies for Antisense Oligonucletotide Therapeutics, CRC Press, Boca Raton, FL, 1995, pp. 199–221.

[20] L. Leserman, M.C. Woodle, Liposomal antisense oligonucleotide therapeutics, in: D.D. Lasic, D. Papahadjopoulos (Eds.), Medical Applications of Liposomes, Elsevier Science B.V., Amsterdam, 1998, pp. 429–449.

[21] S.C. Semple, S.K. Klimuk, T.O. Harasym, M.J. Hope, Lipid-based formulations of antisense oligonucleotides for systemic delivery applications, Methods Enzymol. 313 (2000) 322–341.

[22] D.C. Litzinger, Limitations of cationic liposomes for antisense oligonucleotide delivery in vivo, J. Liposome Res. 7 (1997) 51–61.

[23] P.C. Gokhale, V. Soldatenkov, F.H. Wang, A. Rahman, A. Dritschilo, U. Kasid, Antisense raf oligodeoxyribonucleotide is protected by liposomal encapsulation and inhibits Raf-1 protein expression in vitro and in vivo: implication for gene therapy of radioresistant cancer, Gene Ther. 4 (1997) 1289–1299.

[24] C.F. Bennett, J.E. Zuckerman, D. Kornbrust, H. Sasmor, J.M. Leeds, S.T. Crooke, Pharmacokinetics in mice of a [^{3}H]-labeled phosphorothioate oligonucleotide formulated in the presence and absence of a cationic lipid, J. Control. Release 41 (1996) 121–130.

[25] D.V. Devine, K. Wong, K. Serrano, A. Chonn, P.R. Cullis, Liposome–complement interactions in rat serum: implications for liposome survival studies, Biochim. Biophys. Acta 1191 (1994) 43–51.

[26] A. Chonn, P.R. Cullis, D.V. Devine, The role of surface charge in the activation of the classical and alternative pathways of complement by liposomes, J. Immunol. 146 (1991) 4234–4241.

[27] C. Plank, K. Mechtler, F.C. Szoka Jr., E. Wagner, Activation of the complement system by synthetic DNA complexes: a potential barrier for intravenous gene delivery, Hum. Gene Ther. 7 (1996) 1437–1446.

[28] M.S. Webb, D. Saxon, F.M. Wong, H.J. Lim, Z. Wang, M.B. Bally, L.S. Choi, P.R. Cullis, L.D. Mayer, Comparison of different hydrophobic anchors conjugated to poly(ethylene glycol): effects on the pharmacokinetics of liposomal vincristine, Biochim. Biophys. Acta 1372 (1998) 272–282.

[29] S. Wang, R.J. Lee, G. Cauchon, D.G. Gorenstein, P.S. Low, Delivery of antisense oligodeoxyribonucleotides against the human epidermal growth factor receptor into cultured KB cells with liposomes conjugated to folate via polyethylene glycol, Proc. Natl. Acad. Sci. USA 92 (1995) 3318–3322.

[30] E.L. Wickstrom, T.A. Bacon, A. Gonzalez, D.L. Freeman, G.H. Lyman, E. Wickstrom, Human promyelocytic leukemia HL-60 cell proliferation and c-myc protein expression are inhibited by an antisense pentadecadeoxynucleotide targeted against c-myc mRNA, Proc. Natl. Acad. Sci. USA 85 (1988) 1028–1032.

[31] C.F. Bennett, T.P. Condon, S. Grimm, H. Chan, M.Y. Chiang, Inhibition of endothelial cell adhesion molecule expression with antisense oligonucleotides, J. Immunol. 152 (1994) 3530–3540.

[32] S.M. Stepkowski, Y. Tu, T.P. Condon, C.F. Bennett, Blocking of heart allograft rejection by intercellular adhesion molecule-1 antisense oligonucleotides alone or in combination with other immunosuppressive modalities, J. Immunol. 153 (1994) 5336–5346.

[33] M.J. Hope, R. Nayar, L.D. Mayer, P.R. Cullis, Reduction of liposome size and preparation of unilamellar vesicles by extrusion techniques, in: G. Gregoriadis (Ed.), Liposome Preparation and Related Techniques, CRC Press, Boca Raton, FL, 1993, pp. 123–139.

[34] S.K. Klimuk, S.C. Semple, P.N. Nahirney, M.C. Mullen, C.F. Bennett, P. Scherrer, M.J. Hope, Enhanced anti-inflammatory activity of a liposomal intercellular adhesion molecule-1 antisense oligodeoxynucleotide in an acute model of contact hypersensitivity, J. Pharm. Exp. Ther. 292 (2000) 480–488.

[35] P.R. Dash, M.L. Read, L.B. Barrett, M.A. Wolfert, L.W. Seymour, Factors affecting blood clearance and in vivo distribution of polyelectrolyte complexes for gene delivery, Gene Ther. 6 (1999) 643–650.

[36] C.R. Dass, M.A. Burton, Lipoplexes and tumours. A review, J. Pharm. Pharmacol. 51 (1999) 755–770.

[37] M.A. Monck, A. Mori, D. Lee, P. Tam, J.J. Wheeler, P.R. Cullis, P. Scherrer, Stabilized plasmid-lipid particles: pharmacokinetics and plasmid delivery to distal tumors following intravenous injection, J. Drug Target. 7 (2000) 439–452.

[38] A.L. Bailey, P.R. Cullis, Modulation of membrane fusion by asymmetric transbilayer distributions of amino lipids, Biochemistry 33 (1994) 12573–12580.

[39] P.A. Aarts, O.L. Gijeman, J.M. Kremer, P.H. Wiersema, Dynamics of phospholipid aggregation in ethanol–water solutions, Chem. Phys. Lipids 19 (1977) 267–274.

[40] J.W. Holland, C. Hui, P.R. Cullis, T.D. Madden, Poly(ethylene glycol)-lipid conjugates regulate the calcium-induced fusion of liposomes composed of phosphatidylethanolamine and phosphatidylserine, Biochemistry 35 (1996) 2618–2624.

[41] P.R. Harrigan, M.J. Hope, T.E. Redelmeier, P.R. Cullis, Determination of transmembrane pH gradients and membrane potentials in liposomes, Biophys. J. 63 (1992) 1336–1345.

[42] J.J. Wheeler, L. Palmer, M. Ossanlou, I. MacLachlan, R.W. Graham, Y.P. Zhang, M.J. Hope, P. Scherrer, P.R. Cullis, Stabilized plasmid-lipid particles: construction and characterization, Gene Ther. 6 (1999) 271–281.

[43] S.C. Semple, A. Chonn, P.R. Cullis, Interactions of liposomes and lipid-based carrier systems with blood proteins: Relation to clearance behaviour in vivo, Adv. Drug Deliv. Rev. 32 (1998) 3–17.

[44] R.L. Juliano, S. Akhtar, Liposomes as a drug delivery system for antisense oligonucleotides, Antisense Res. Dev. 2 (1992) 165–176.

[45] O. Zelphati Jr., F.C. Szoka, Liposomes as a carrier for intracellular delivery of antisense oligonucleotides: a real or magic bullet?, J. Control. Release 41 (1996) 99–119.

[46] T. Friedmann, Overcoming the obstacles to gene therapy, Sci. Am. 276 (1997) 96–101.

[47] A.R. Thierry, A. Dritschilo, Intracellular availability of unmodified, phosphorothioated and liposomally encapsulated oligodeoxynucleotides for antisense activity, Nucleic Acids Res. 20 (1992) 5691–5698.

[48] A.R. Thierry, A. Rahman, A. Dritschilo, Liposomal delivery as a new approach to transport antisense oligonucleotides, in: R.P. Erickson, J.G. Izant (Eds.), Gene Regulation: Biology of Antisense RNA and DNA, Raven Press Ltd., New York, 1992, pp. 147–161.

[49] A. Chonn, S.C. Semple, P.R. Cullis, Association of blood proteins with large unilamellar liposomes in vivo. Relation to circulation lifetimes, J. Biol. Chem. 267 (1992) 18759–18765.

[50] A.M. Tari, S.D. Tucker, A. Deisseroth, G. Lopez-Berestein, Liposomal delivery of methylphosphonate antisense oligodeoxynucleotides in chronic myelogenous leukemia, Blood 84 (1994) 601–607.

[51] A.M. Tari, C. Stephens, M. Rosenblum, G. Lopez-Berestein, Pharmacokinetics, tissue distribution, and safety of P-ethoxy oligonucleotides incorporated in liposomes, J. Liposome Res. 8 (1998) 251–264.

[52] S. Huebner, B.J. Battersby, R. Grimm, G. Cevc, Lipid–DNA complex formation: reorganization and rupture of lipid vesicles in the presence of DNA as observed by cryoelectron microscopy, Biophys. J. 6 (1999) 3158–3166.

[53] S. Batzri, E.D. Korn, Single bilayer liposomes prepared without sonication, Biochim. Biophys. Acta 298 (1973) 1015–1019.

[54] S.K. Hobbs, W.L. Mosky, F. Yuan, W.G. Roberts, L. Griffith, V.P. Torchilin, R.K. Jain, Regulation of transport pathways in tumor vessels: Role of tumor type and microenvironment, Proc. Natl. Acad. Sci. USA 95 (1998) 4607–4612.

[55] S.K. Klimuk, S.C. Semple, P. Scherrer, M.J. Hope, Contact hypersensitivity: a simple model for the characterization of disease-site targeting by liposomes, Biochim. Biophys. Acta 1417 (1999) 191–201.

[56] D.D. Stuart, G.Y. Kao, T.M. Allen, A novel, long-circulating, and functional liposomal formulation of antisense oligodeoxynucleotides targeted against MDR1, Cancer Gene Ther. 7 (2000) 466–475.

[57] D.D. Stuart, T.M. Allen, A new liposomal formulation for antisense oligodeoxynucleotides with small size, high incorporation efficiency and good stability, Biochim. Biophys. Acta 1463 (2000) 219–229.